Carboxylated Nanocrystalline Cellulose from *Salix psammophila* Prepared by Sulfuric Acid Hydrolysis Combined with 2,2,6,6-tetramethylpiperidine-1-oxyl (TEMPO)-oxidation

Yuan Zhong,[a] Xueyi Gao,[a,+] Wanqi Zhang,[b] Xue Wang,[c] and Kebing Wang *

Salix psammophila (SP) is an important sand plant, and could be utilized to develop high-value products. In this work, SP was used as raw material and cellulose nanocrystals (CNC) were prepared by hydrolysis in 64 wt% sulfuric acid (H_2SO_4) solution, and then, TEMPO/NaBr/NaClO system was used to oxidize CNC to obtain TEMPO-oxidation-cellulose nanocrystals (TOCNC). Fourier transform infrared analysis (FTIR) revealed that after oxidation, there were obvious carboxyl functional groups. Scanning electron microscopy (SEM) showed that both CNC and TOCNC were agglomerated. Under atomic force microscope (AFM) and transmission electron microscopy (TEM), CNC and TOCNC presented short rod fibers, average diameters of 23 nm and 21 nm and average lengths of 213 nm and 165 nm, respectively. X-ray photoelectron spectroscopy analysis (XPS) showed that TOCNC generated a new energy spectrum peak at 289.06 eV, which was the peak of C=O in the carboxyl group. The crystallinity of the CNC and TOCNC were 70.8% and 26.9%, respectively.

DOI: 10.15376/biores.17.1.1373-1384

Keywords: Sand shrub; Sulfuric acid; TEMPO-mediated oxidation; CNC

*Contact information: a: College of Science, Inner Mongolia Agriculture University, Hohhot 010018, China; b: College of Materials Science and Art Design, Inner Mongolia Agricultural University, Hohhot 010018, China; c: College of Science, Inner Mongolia Agriculture University, Hohhot 010018, China; [+]These authors contributed equally; *Corresponding author: wkb0803@163.com*

INTRODUCTION

Salix psammophila is a type of sand shrub, which is broad-leaved and has porous wood. It is an important plant for windbreak and sand fixation in arid areas, and one of the characteristic plants for afforestation in sandy land in Inner Mongolia. It has the characteristics of rapid growth, simple reproduction, high survival rate, and resistance to drought (Bao and Zhang 2012). *Salix psammophila* should be stubbled regularly to keep its growth vitality, thus producing a high amount of waste. The simple incineration of waste *S. psammophila* not only fails to make rational use of calorific value, but also causes serious environmental pollution such as dust, sulfur oxides, and nitrogen oxides. Therefore, it is particularly important to improve the application of waste sand ash resources and realize the "turning waste into treasure" of waste sand ash resources (Nguyen and Nguyen 2019). *Salix psammophila* contains 36.9% cellulose, 35.0% hemicellulose, 24.8% lignin, a small amount of ash, tannin, and lipids, *etc.* (Huang 2014). Due to the high cellulose content in *S. psammophila*, it is often used in pulp and papermaking, chemical raw materials, biomass fuel, and fiberboard.

Nanocellulose is a fine structure cellulose with a diameter of 1 to 100 nm obtained by hydrolysis or mechanical treatment of cellulose. Nanocellulose types can be divided into bacterial nanocellulose (BNC) (Ju *et al.* 2020), cellulose nanocrystalline (CNC) (Shao *et al.* 2017), and cellulose nanofibrillated (CNF) (Besbes *et al.* 2011). There are three methods for conventional preparation of nanocellulose. The first method is obtained by pure chemical pretreatment, that is, removing the amorphous zone of cellulose with sulfuric acid, phosphoric acid (Vanderfleet *et al.* 2018), hydrochloric acid (Shang *et al.* 2019), and other acids. The second method involves breaking the cellulose itself by mechanical stripping. Representative instruments include an ultrasonic crusher (Jiang *et al.* 2021), high-pressure homogenizer (Park *et al.* 2019), and micro-jet nanoscale homogenizer, *etc.* The third method is to pretreat cellulose through sodium periodate (Sun *et al.* 2015), TEMPO (De Castro *et al.* 2018), nitrogen oxide, N-Hydroxyphthalimide (NHPI), and other oxidation systems (Zhou *et al.* 2014) to change the functional groups of cellulose, thus achieving specific good physical and chemical properties. After such chemical treatments, nanocellulose with different chemical properties can be obtained through mechanical treatment. As a renewable nanomaterial, nanocellulose has been widely used in the fields of medicine, food, papermaking, composite materials, *etc.* (Kaushik and Singh 2011).

The 2,2,6,6-tetramethylpiperidin-1-oxyl (TEMPO) radical belongs to the nitrosyl radical class and is a type of ring compound with stable nitrogen oxygen radical structure (Isogai *et al.* 2011). TEMPO is characterized by high oxidation efficiency, mild conditions, and a high degree of selectivity (Bragd *et al.* 2004). TEMPO can selectively oxidize the primary hydroxyl group at the position C_6 of cellulose (Okita *et al.* 2009), starch (Boccia *et al.* 2020; Hao *et al.* 2020), chitin (Fan *et al.* 2008; Ye *et al.* 2021), and other polysaccharide long chain macromolecules, turning them into carboxyl groups. Therefore, TEMPO is popular in the field of modification of oxidized polysaccharide compounds (Bragd *et al.* 2000; Saito and Isogai 2004; Ma *et al.* 2020).

In the present work, the previously reported isolation of *Salix psammophila* microcrystalline cellulose (SP-Mic-C), SP-Mic-C was used as raw material to prepare CNC by hydrolyzed with sulfuric acid. Then, TOCNC was prepared by TEMPO/NaBr/NaClO mediated oxidation, and the products were characterized with a view to make subsequent aerogel and hydrogel materials on the basis of this material.

EXPERIMENTAL

Materials and Methods

Materials and reagent

Salix psammophila specimens were collected from Kabuki Desert of Ordos, China. Samples were cleaned with water, dried, and crushed; 100 to 120 mesh powder was measured for reserve. The following materials and reagents were used in the experiment: nitric acid (HNO_3), hydrochloric acid（HCl), sulfuric acid (H_2SO_4) (Sinopharm Chemical Reagents Co., Ltd., Beijing, China); sodium chlorite ($NaClO_2$) 80% TEMPO, sodium bromide (NaBr) (McLean Chemical Reagents Ltd., Shanghai, China); anhydrous ethanol (C_2H_5OH), sodium hypochlorite (NaClO), sodium hydroxide (NaOH) (Tianjin Kemao Chemical Reagent Co., Ltd., Tianjing, China); glacial acetic acid(CH_3COOH) (Tianjin Fuchen Chemical Reagent Co., Ltd., Tianjing, China); potassium hydroxide(KOH) (Tianjin Jinhuitai Subchemical Reagent Co., Ltd., Tianjing, China). The above drugs were analytically pure.

Preparation of S. psammophila microcrystalline cellulose

The extraction of cellulose from *Salix* microcrystalline was based on the method described in a previous paper (Zhong *et al.* 2020). 10 g *S. psammophila* was weighed and heated in distilled water at 1:60 g/mL for 1 h at 80 °C. Impurities and some water-soluble components were removed by filtration, and the yield was 87%. The HNO_3-C_2H_5OH solution (1:3 V/V, 1:43 g/mL) was weighed and placed in a three-necked flask, condensed, and refluxed at 90 °C. After the sample was removed, it was washed to neutral with distilled water and anhydrous ethanol and dried at 105 °C with constant weight. After drying, it was added into 7.5 wt% NaClO (1:20 g/mL), adjusted to pH of 3 to 4 with CH_3COOH, reacted at 75 °C for 3 h, washed with distilled water and anhydrous ethanol to neutral, and dried at 60 °C to constant weight. The bleached samples were then placed in 10% KOH (1:20 g/mL) solution, magnetically stirred at 75 °C for 2 h, washed to neutral, and dried to constant weight at 60 °C. Finally, 8 wt% HCl solution (1:20 g/mL) was hydrolyzed at 90 ℃ for 1.5 h. The product was successively washed with distilled water and anhydrous ethanol to neutral. After drying, the sample was named SP-Mic-C.

Preparation of cellulose nanocrystalline by sulfuric acid hydrolysis

1 g of SP-Mic-C was accurately weighed, and was put into a 20 mL conical flask, with 10 mL of 64 wt% H_2SO_4 solution, and was stirred at 45 °C for 45 min. Then, the solution was diluted with 900 mL distilled water. It was allowed to stand overnight, and then the supernatant was poured out. A certain amount of distilled water was added again, and this process was repeated 2 to 3 times. A dialysis bag (8000 to 14000 MW) was used for dialysis until the pH was nearly neutral (Ping and Hsieh 2012). The sample was named CNC after freeze-drying, and the yield was about 73.9%.

Preparation of TEMPO-oxidation-cellulose nanocrystalline by TEMPO oxidation

1 g of CNC was added to the flask, 100 mL of water was added, and 0.032 g TEMPO and 0.603 g NaBr were then added.

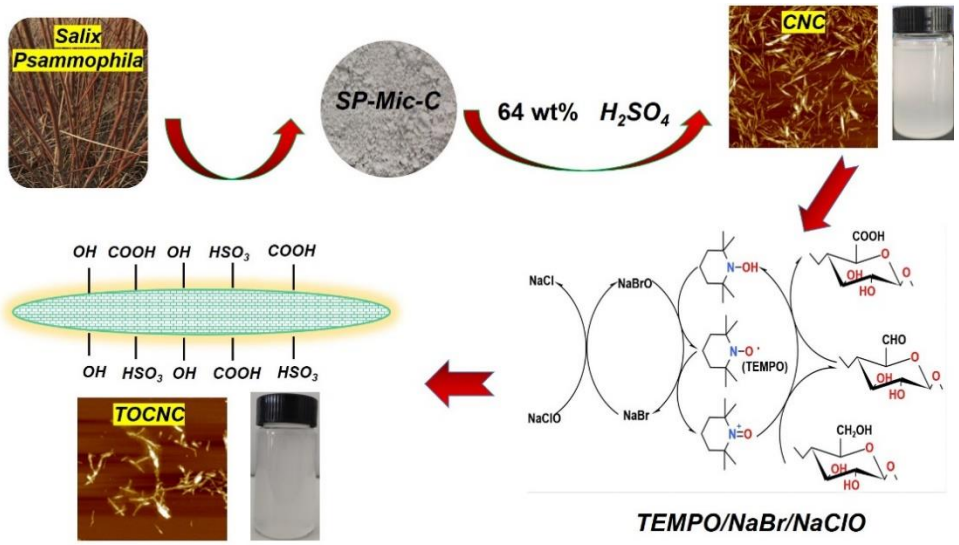

Fig. 1. TOCNC preparation process and mechanism diagram

After stirring at 60 °C for 30 min, 20 mL NaClO solution (10 wt%) was added, and 0.5 M NaOH solution was used to adjust the pH of the solution to 10.0~10.5 until the end of the reaction. Anhydrous ethanol (20 mL) was used to quench the reaction. The solution was dialyzed to neutral and freeze-dried. The sample was named TOCNC with a yield of approximately 21.7%. The TOCNC preparation process is shown in Fig. 1.

Analysis Methods

Scanning electron microscopy (SEM)

Scanning electron microscopy (SEM) (Hitachi 4800; Hitachi Limited, Tokyo, Japan) was used to observe the changes of the sample surface during the process from raw material to cellulose. The scanning electron microscope (SEM) was operated at an accelerating voltage of 10 kV. A small number of samples was placed on conductive adhesive. Then they were gold sprayed (Small ion sputtering instrument; Beijing Zhongke Instrument Co., Ltd., Beijing, China), and their morphology was observed.

Transmission electron microscopy (TEM)

For TEM, a FEI Tecnai S-200kV Twin field emission high resolution transmission electron microscope was used (Thermo Fisher Scientific, Waltham, MA, USA). The sample was diluted with anhydrous ethanol, dried in copper mesh and tested.

Atomic force microscope analysis (AFM)

The test was performed with a Bruker atomic force microscope (Dimension Icon; Bruker Corporation, Madison, WI, USA). A certain amount of nanocellulose was diluted with distilled water and stirred evenly. A drop of nanocellulose suspended liquid was placed on the mica sheet, and the sample with a range of 2 μm × 2 μm. Photoshop CC 2019 (Adobe Systems Incorporated, 2019, State of California, USA) was used to measure and analyze the diameter and length of the nanocellulose.

Fourier transform infrared spectroscopy (FTIR)

The FTIR spectra were measured using a Perkin Elmer 65 (Perkin Elmer Instruments Co., Ltd., Waltham, MA, USA). The experimental parameters included a range of 4000 to 600 cm^{-1}. The cumulative number of scans was 32, and the resolution was 1 cm^{-1}.

X-ray photoelectron spectroscopy (XPS)

Elemental analysis of the material surface was performed with the Thermo Scientific Escalab 250XI (Thermo Fisher Technologies, Waltham, MA, USA) photo-electron spectrometer, and the radiation source was Al-Kα.

Thermo gravimetric analysis (TGA)

The TGA experiments were performed on an HCT-1 integrated thermal analyser (Beijing Hengjiu Scientific Instrument Factory, Beijing, China). The samples were analysed in N_2 atmosphere with a pressure of 0.3 MPa, a flow rate of 20 mL/min, a heating rate of 10 °C/min, and a temperature range of 25 to approximately 800 °C.

X-ray diffraction (XRD)

Tests were run in an X-ray diffractometer (Empyrean Alpha-1, Shanghai SIBG Instrument System Co., Ltd., Shanghai, China). Test conditions were the following: Cu Ka

radiation at a generator voltage of 40 kV and current of 40 mA; radiation angle for $2\theta = 5°$ to approximately 80°, with a step size of 0.017° and a count time of 4.5 min. The crystallinity index of samples was calculated by the Segal equation (Segal *et al.* 1959), listed here as Eq. 1,

$$CrI = (I_2 - I_1) / I_2 \times 100\% \quad (1)$$

where CrI is the crystallinity index (%), I_2 is the crystalline peak intensity around $2\theta = 20°$, and I_1 is the amorphous intensity of the background scattered measure around $2\theta = 18°$.

RESULTS AND DISCUSSION

The Sample Appearance

Figure 2 shows the nanocellulose prepared in this study. The CNC obtained after H_2SO_4 treatment was milky white. In addition, both nanocellulose solutions were pale blue at very low concentrations, and the dilute suspensions remained stable within a month.

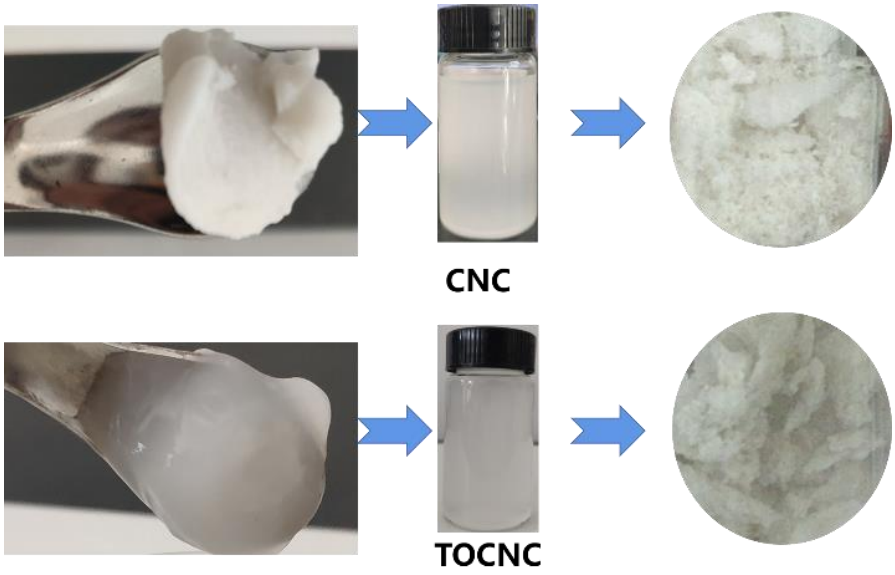

Fig. 2. Morphology (Left, after centrifugal; Right, after freeze drying) of CNC and TOCNC

Scanning Electron Microscopy (SEM)

The SP-Mic-C, CNC, and TOCNC SEM images are shown in Fig. 3. As can be seen from Fig. 3a, SP-Mic-C had a long rod-like structure. SP-Mic-C had been hydrolyzed by H_2SO_4. The relatively uniform size of particles of CNC is attributed to the rapid hydrolysis of the amorphous cellulose regions by the concentrated sulfuric acid (Fig. 3b). Based on the images shown in the micrographs, the CNC particles appear to have been reunited into a layered structure, such that it was no longer possible to distinguish between single nanorods. Compared with CNC, TOCNC (Fig. 3c) showed a smoother layer surface and exhibited smaller flocs and fault. After TEMPO oxidation treatment of CNC, more hydroxyl and carboxyl groups on the surface of the oxidized nanocellulose enable it to absorb water and swell, and the bloated nanocellulose will form more hydrogen bonds after freeze-drying treatment, resulting in a denser structure.

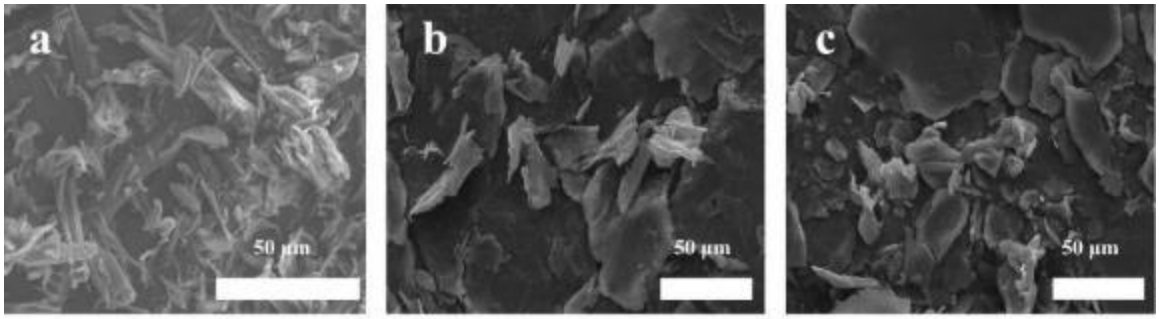

Fig. 3. SEM images of SP-Mic-C (a), CNC (b), and TOCNC (c)

FTIR Analysis

Figure 4(a) shows the FTIR spectra of SP-Mic-C, CNC, and TOCNC. The wide absorption band at 3340 cm^{-1} is the stretching vibration peak of -OH. The peak of $-CH_3$ near 2900 to 2971 cm^{-1} is the C-H stretching vibration (Kumar *et al*. 2019); 1600 cm^{-1} is the asymmetric contraction vibration of $-COO^-$ (Mendoza *et al.* 2019), which does not appear in the SP-Mic-C and CNC. However, after TEMPO oxidation treatment, the TOCNC exhibited carboxyl functional groups, indicating that the preparation of TOCNC was successful. Near 1434 cm^{-1} is the type for $-CH_2$ bending vibration peak (Luo and Wang 2018). This indicates that samples remained as the cellulose I type crystal type, and there was no structural change; 1032 cm^{-1} is the C-O stretching vibration peak of cellulose. It also is the characteristic absorption peak of cellulose (Yang *et al.* 2015).

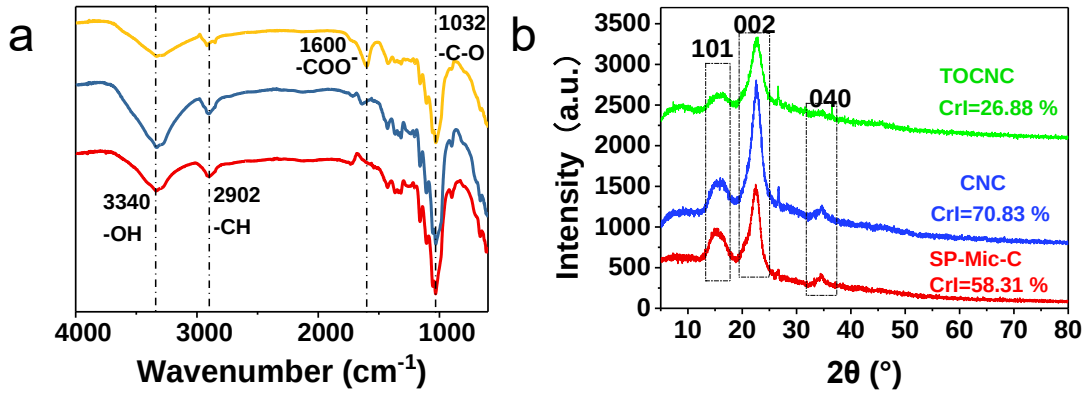

Fig. 4. FTIR analysis (a) and XRD patterns (b) of SP-Mic-C, CNC, and TOCNC

XRD Analysis

Figure 4(b) shows the XRD diagram for SP-Mic-C, CNC, and TOCNC; the peaks at 2θ = 16°, 22°, and 34° were associated with the (101), (002), and (040) crystal planes for the cellulose type I crystalline structure (Yan *et al.* 2019). After the H_2SO_4 hydrolysis, CNC crystallinity of 70.8% was far higher than SP-Mic-C, 58.3%. After TEMPO oxidation, the crystallinity of TOCNC dropped sharply to 26.9%. This can be attributed to β-elimination reaction and the degradation reaction. (Henriksson *et al*. 2007).

AFM Analysis

The atomic force microscope is an instrument for imaging samples using optical lever technology. The method has a good resolution for examination of nanoscale materials. Figure 5(a, b) is the atomic force microscope diagram of CNC and TOCNC,

from which it can be seen that both nanocellulose are short rods, which is consistent with the effect shown by TEM, and the image is clearer. From Fig. 5 (a1, a2, b1, b2), which shows length and width distribution of CNC and TOCNC, the average diameter of nanocellulose decreased from 23 nm to 21 nm, and the average length decreased from 213 nm to 165 nm. The experimental data demonstrates that preparation of the TEMPO-oxidized cellulose involved a certain extent of degradation, and the introduction of carboxyl groups also improved the dispersion of the particles.

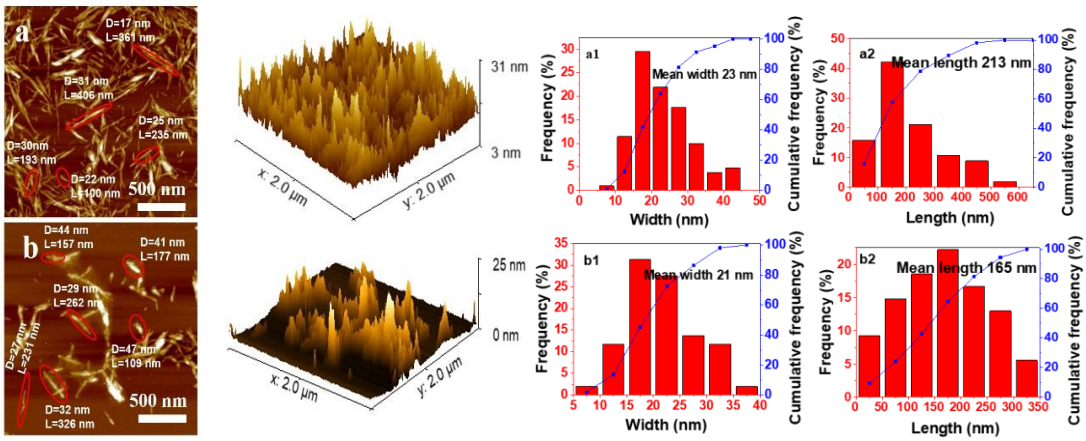

Fig. 5. AFM images of CNC (a) and TOCNC (b): width and Length distribution of CNC (a1, a2) and TOCNC (b1, b2)

TEM Analysis

The TEM method directly examines thin samples with the help of electrons to form an image. It can be seen from Fig. 6 that the CNC had a fine rod-like structure, and after TEMPO-mediated treatment, the diameter and length of TOCNC were slightly lower than those of CNC.

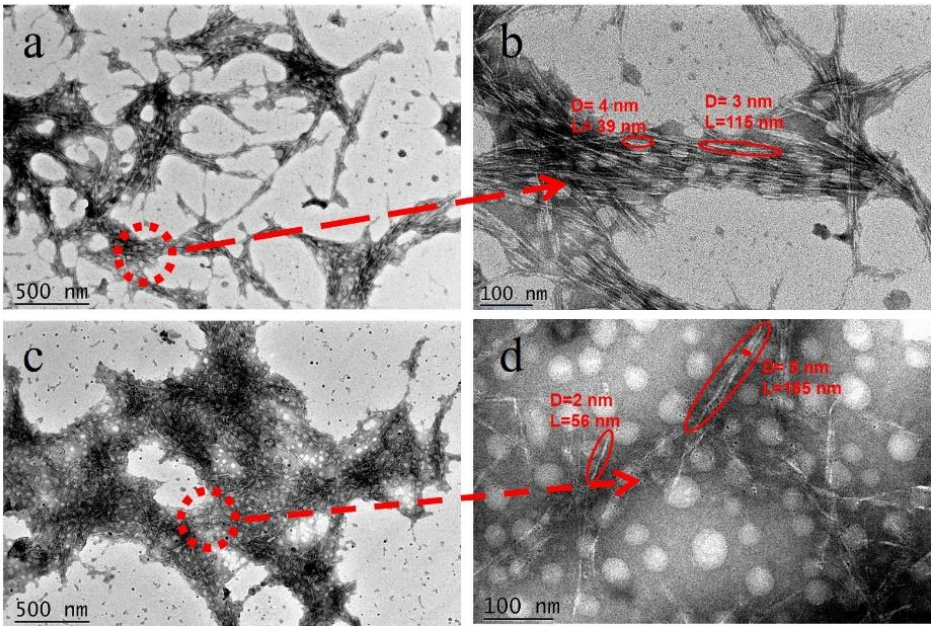

Fig. 6. TEM images of CNC (a, b) and TOCNC (c, d)

Both CNC and TOCNC were subject to relatively obvious agglomeration phenomena. Because the surface of nanocellulose is rich in hydroxyl groups, it is easy to form hydrogen bonds. The hydrogen bonds between cellulose and van der Waals forces cause the formation of nanocellulose fiber bundle agglomerations.

TGA Analysis

The SP-Mic-C, CNC, and TOCNC TG (Fig. 7a) and DTG (Fig. 7b) analysis diagram is shown in Fig. 7. Moisture becomes volatilized usually within the range 50 to 150 °C for the samples. The CNC exhibited the largest thermal decomposition temperature of 263 °C, which was lower than the TOCNC maximum thermal decomposition temperature of 296 °C. The maximum thermal decomposition temperature of SP-Mic-C was 354 °C. Thus, the TOCNF decomposition was nearly 70 °C lower than that of SP-Mic-C. There are two reasons for this. First, this was because the two kinds of nanocellulose have different particle sizes, surface and degree of polymerization, which leads them to have greater exposure of surface area; Second, it is caused by the introduction of sulfonic acid groups and acid hydrolysis and reduction of the degree of polymerization of cellulose chains (Rosa *et al.* 2010).

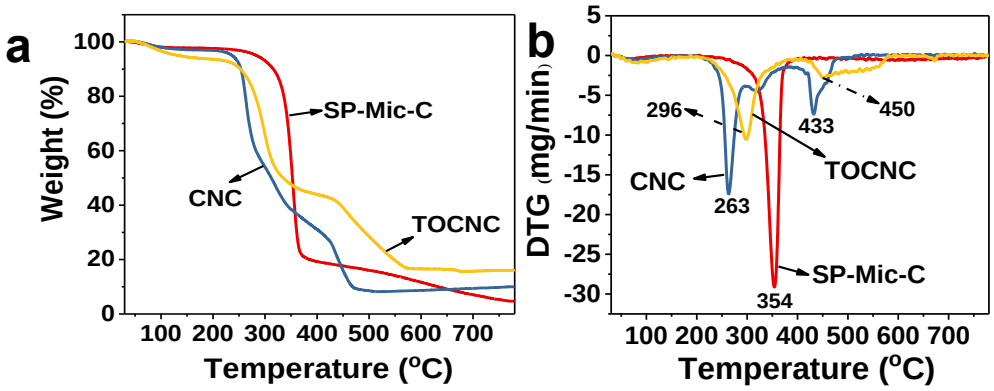

Fig. 7. TG (a) and DTG (b) analysis of SP-Mic-C, CNC, and TOCNC

XPS Analysis

X-ray photoelectron spectroscopy is one of the technical means for qualitative and quantitative analysis of compounds by photoelectric effect (Zheng *et al.* 2013). Figure 8 shows the XPS analysis curve of CNC and TOCNC. Table 1 shows the relative content ratio of each element in XPS. It can be seen from Table 1 that both groups of samples were composed of a large amount of C, O, and a small amount of sulfur and other elements. The oxygen-carbon ratio changed from 30.79% of CNC to 50.51% of TOCNC. This showed that the TEMPO-oxidation process increased the oxygen-carbon ratio of the sample. The sulfur content in CNC also decreased from 0.61% to 0.32% of TOCNC (Yang *et al.* 2015), which was attributed to the degradation of cellulose by the alkaline TEMPO/NaBr/NaClO oxidation system. Compared with CNC, the S2P peak of TOCNC was remarkably reduced. The binding energy and chemical shift of the C1S peak on the surface of CNC can explain the change of the sample structure to some extent. Under the influence of electron-withdrawing groups, the density of electron cloud around carbon atom decreases, the shielding effect weakens, and the electron binding energy increases. The three energy spectrum peaks of CNC and TOCNC around 284.8 eV, 286.5 eV, and 288.1 eV correspond to C-C/C-H, C-OH/C-O, and C-O-C, respectively. For TOCNC, a new energy spectral peak

is generated at 289.06 eV, which is the peak of C=O in the carboxyl group. Figure 8 (a, d) indicates that the oxidation of nanocellulose gave rise to a carboxyl group.

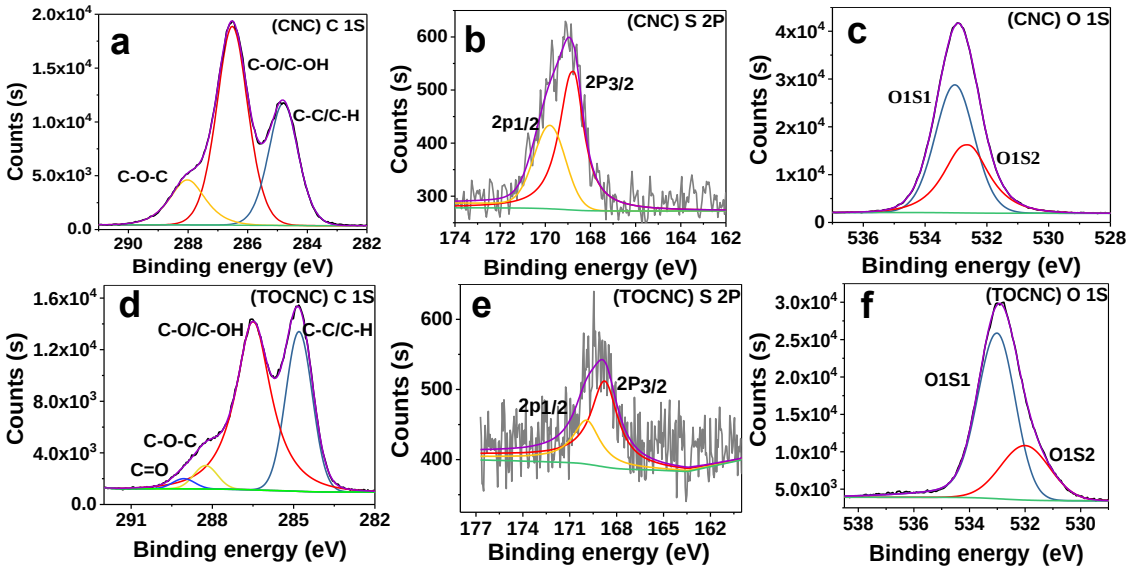

Fig. 8. XPS analysis of CNC (a, b, c) and TOCNC (d, e, f)

Table 1. Comparison Data between CNC and TOCNC

Comparison Type	CNC	TOCNC
Yield (%)	73.89	21.74
Crystallinity (%)	70.83	26.88
Average Diameter (nm)	23	21
Average Length (nm)	213	165
Temperature of Maximum Thermal Decomposition Rate (°C)	263	296
Relative Oxygen Content in XPS (%)	24.54	31.46
Relative Carbon Content in XPS (%)	74.85	68.22
Relative Sulfur Content in XPS (%)	0.61	0.32

CONCLUSIONS

1. TEMPO-oxidized-cellulose nanocrystals (TOCNC) with carboxyl functional groups were prepared from *Salix psammophila* microcrystalline cellulose (SP-Mic-C) by sulfuric acid hydrolysis and 2,2,6,6-tetramethylpiperidin-1-oxyl (TEMPO) oxidation.
2. Cellulose nanocrystals (CNC) and TEMPO-oxidized cellulose nanocrystals (TOCNC) presented short rod fibers, average diameters of 23 nm and 21 nm, and average lengths of 213 nm and 165 nm, respectively.
3. The crystallinities of the CNC and TOCNC were 70.8% and 26.9%, respectively.
4. The successful preparation of TOCNC provides a promising way for the utilization of abandoned agricultural and forestry resources and provides a certain reference for the study of abandoned agricultural and forestry resources.

ACKNOWLEDGMENTS

The authors acknowledge support from the Research Start-up Fee for Introducing Talents (RZ1900003332), Inner Mongolia Higher Education Scientific Research Project (NJZY17063), and Inner Mongolia Agricultural University Doctoral Research Start-up Fund (BJ06-57).

REFERENCES CITED

Bao, Y., and Zhang, G. (2012). "Study of adsorption characteristics of methylene blue onto activated carbon made by *Salix psammophila*," *Energy Procedia* 16(1), 1141-1146. DOI: 10.1016/j.egypro.2012.01.182

Besbes, I., Alila, S., and Boufi, S. (2011). "Nanofibrillated cellulose from TEMPO-oxidized eucalyptus fibres: Effect of the carboxyl content," *Carbohydrate Polymers* 84(3), 975-983. DOI: 10.1016/j.carbpol.2010.12.052

Boccia, A. C., Scavia, G., and Schizzi, I. (2020). "Biobased cryogels from enzymatically oxidized starch: Functionalized materials as carriers of active molecules," *Molecules* 25(11), 2557. DOI: 10.3390/molecules25112557

Bragd, P. L., Besemer, A, C., and van, Bekkum. H. (2000). "Bromide-free TEMPO-mediated oxidation of primary alcohol groups in starch and methyl α-D-glucopyranoside," *Carbohydrate Research* 328(3), 355-363. DOI: 10.1016/S0008-6215(00)00109-9

Bragd, P. L., Van, Bekkum. H., and Besemer, A. C. (2004). "TEMPO-mediated oxidation of polysaccharides: Survey of methods and applications," *Topics in Catalysis* 27(1-4), 49-66. DOI: 10.1023/B:TOCA.0000013540.69309.46

De Castro, D. O., Tabary, N., and Martel, B., (2018). "Controlled release of carvacrol and curcumin: Bio-based food packaging by synergism action of TEMPO-oxidized cellulose nanocrystals and cyclodextrin," *Cellulose*, 25(2), 1249-1263. DOI: 10.1007/s10570-017-1646-6

Fan, Y., Saito, T., and Isogai, A. (2008). "Chitin nanocrystals prepared by TEMPO-mediated oxidation of α-chitin" *Biomacromolecules* 9(1), 192-198. DOI:10.1021/bm700966g

Hao, J., Wu, F., and Tang, R. (2020). "Preparation of 1,4-linked α-D-glucuronans from starch with 4-acetamide-TEMPO/$NaClO_2$/NaClO system," *International Journal of Biological Macromolecules* 151, 740-746. DOI: 10.1016/j.ijbiomac.2020.02.211

Henriksson, M., Henriksson, G., and Berglund, L. A. (2007). "An environmentally friendly method for enzyme-assisted preparation of microfibrillated cellulose (MFC) nanofibers," *European Polymer Journal* 43(8), 3434-3441 DOI: 10.1016/j.eurpolymj.2007.05.038

Huang, M.X. (2014). *Study on the Preparation Process of Microcrystalline Cellulose From Salix psammophila*, Master's Thesis, Zhengzhou University, Zhengzhou, China.

Isogai, A., Saito, T., and Fukuzumi, H. (2011). "TEMPO-oxidized cellulose nanofibers," *Nanoscale* 3(1), 71-85. DOI: 10.1039/C0NR00583E

Jiang, S., Farooq, A., and Han, F. (2021). "Investigation of a widely applicable process for extracting carboxyl-rich cellulose nanocrystal (CNC)," *Fibers and Polymers* 2021(3), 1-11. DOI: 10.1007/s12221-021-0279-4

Ju, S. Y., Yu, H. L., and Ji, L. (2020). "Preparation and characterization of bacterial nanocellulose-based composite membranes," *Science of Advanced Materials* 12(6), 802-809. DOI: 10.1166/sam.2020.3742

Kaushik, A., and Singh, M. (2011). "Isolation and characterization of cellulose nanofibrils from wheat straw using steam explosion coupled with high shear homogenization," *Carbohydrate Research* 346(1), 76-85. DOI: 10.1016/j.carres.2010.10.020

Kumar, R., Kumari, S., and Surah, S. S. (2019). "A simple approach for the isolation of cellulose nanofibers from banana fibers," *Materials Research Express* 6(10), article no. 105601. DOI: 10.1088/2053-1591/ab3511

Luo, X., and Wang, X. (2017). "Preparation and characterization of nanocellulose fibers from NaOH/urea pretreatment of oil palm fibers," *BioResources* 12(3). DOI: 10.15376/biores.12.3.5826-5837

Ma, H., Huang, Q., and Ren, J. (2020). "Structure characteristics, solution properties and morphology of oxidized yeast β-glucans derived from controlled TEMPO-mediated oxidation," *Carbohydrate Polymers* 250, 116924. DOI: 10.1016/j.carbpol.2020.116924

Mendoza, D. J., Browne, C., and Raghuwanshi, V. S. (2019). "One-shot TEMPO-periodate oxidation of native cellulose," *Carbohydrate Polymers* 226, article no. 115292. DOI: 10.1016/j.carbpol.2019.115292

Nguyen, A., and Nguyen, M. N. (2019). "Straw phytolith for less hazardous open burning of paddy straw," *Scientific Reports* 9(1), article no. 20043. DOI: 10.1038/s41598-019-56735-x

Okita, Y., Saito, T., and Isogai, A. (2009). "TEMPO-mediated oxidation of softwood thermomechanical pulp," *Holzforschung* 63(5), 529-535. DOI: 10.1515/HF.2009.096

Park, N. M., Choi, S., and Oh, J. E. (2019). "Facile extraction of cellulose nanocrystals," *Carbohydrate Polymers* 223, article no. 115114. DOI: 10.1016/j.carbpol.2019.115114

Ping, L., and Hsieh, Y. L. (2012). "Preparation and characterization of cellulose nanocrystals from rice straw," *Carbohydrate Polymers* 87(1), 564-573. DOI: 10.1016/j.carbpol.2011.08.022

Rosa, M. F., Medeiros, E. S., and Malmonge, J. A. (2010). "Cellulose nanowhiskers from coconut husk fibers: Effect of preparation conditions on their thermal and morphological behavior," *Carbohydrate Polymers* 81(1), 83. DOI: 10.1016/j.carbpol.2010.01.059

Saito, T., and Isogai, A. (2004). "TEMPO-mediated oxidation of native cellulose. The effect of oxidation conditions on chemical and crystal structures of the water-insoluble fractions," *Biomacromolecules* 5(5), 1983-1989. DOI: 10.1021/bm0497769

Segal, L., Creely, J. J., and Martin, A. E. (1959). "An empirical method for estimating the degree of crystallinity of native cellulose using the X-ray diffractometer," *Textile Research Journal* 29(10), 786-794. DOI: 10.1177/004051755902901003

Shang, Z., An, X., and Seta, F. T. (2019). "Improving dispersion stability of hydrochloric acid hydrolyzed cellulose nano-crystals," *Carbohydrate Polymers* 222, article no. 115037. DOI: 10.1016/j.carbpol.2019.115037

Shao, C., Wang, M., and Chang, H. (2017). "A self-healing cellulose nanocrystal-poly (ethylene glycol) nanocomposite hydrogel via Diels–Alder click reaction," *ACS Sustainable Chemistry & Engineering* 5(7), 6167-6174. DOI: 10.1021/acssuschemeng.7b01060

Sun, B., Hou, Q., and Liu, Z. (2015). "Sodium periodate oxidation of cellulose nanocrystal and its application as a paper wet strength additive," *Cellulose* 22(2), 1135-1146. DOI: 10.1007/s10570-015-0575-5

Vanderfleet, O. M., Osorio, D. A., and Cranston, E. D. (2018). "Optimization of cellulose nanocrystal length and surface charge density through phosphoric acid hydrolysis," *Philosophical Transactions of the Royal Society A: Mathematical, Physical and Engineering Sciences* 376(2112), article no. 20170041. DOI: 10.1098/rsta.2017.0041

Yan, L., Wang, L., and Gao, S. (2019). "Celery cellulose hydrogel as carriers for controlled release of short-chain fatty acid by ultrasound," *Food Chemistry* 309, article no. 125717. DOI: 10.1016/j.foodchem.2019.125717

Yang, D., Peng, X., and Zhong, L. (2015). "Fabrication of a highly elastic nanocomposite hydrogel by surface modification of cellulose nanocrystals," *RSC Advances* 5(18), 13878-13885. DOI: 10.1039/c4ra10748a

Ye, W., Yokota, S., and Fan, Y. (2021). "A combination of aqueous counter collision and TEMPO-mediated oxidation for doubled carboxyl contents of α-chitin nanofibers," *Cellulose* 1-15. DOI: 10.1007/s10570-021-03676-2

Zheng, G., Cui, Y., and Karabulut, E. (2013). "Nanostructured paper for flexible energy and electronic devices," *MRS Bulletin* 38(4), 320-325. DOI: 10.1557/mrs.2013.59

Zhong, Y., Wang, K. B., Liu, Y. L., and Wang, X. (2020). "Preparation and characterization of *Salix psammophila* cellulose and Mic-cellulose under the pretreatment of two kinds of acid," *J. Phys. Conf. Ser.* 1605(1), article ID 012165. DOI: 10.1088/1742-6596/1605/1/012165

Zhou, L., Wu, H., and Yang, X., (2014). "Selective oxidation of cellulose catalyzed by NHPI/$Co(OAc)_2$ using air as oxidant," *Cellulose* 21(6), 4059-4065. DOI: 10.1007/s10570-014-0413-1

Article submitted: July 2, 2021; Peer-review completed: December 11, 2021; Revised version received and accepted: December 25, 2021; Published: January 7, 2022.
DOI: 10.15376/biores.17.1.1373-1384